AAS 17-610

DEFLECTION ASSESSMENT FOR A GRAVITY TRACTOR SPACECRAFT

Shyam Bhaskaran *

One proposed method to deflect a potential Earth impacting asteroid is via the "gravity tractor" method. Here, a spacecraft, hovering close to an asteroid using ion engines, uses its gravitational pull to change the asteroid?s orbit away from an impacting path. The proposed Asteroid Redirect Robotic Mission was slated to demonstrate the feasibility of this technique on the asteroid 2008EV5, and measure the amount of deflection. In this paper, the questions of how long the tractoring needs to be to cause a measurable deflection, and how the spacecraft can be used to measure it were examined.

INTRODUCTION

The February 2013 impact of a small asteroid over the skies of Chelyabinsk, Russia underscored the threat to Earth from Near Earth Asteroids (NEAs). Although the damage caused from this incident was relatively minor, larger NEAs exist which could potentially cause much more significant harm. In order to mitigate the danger from these objects, several possibilities exist to deflect an asteroid on an Earth impact trajectory. These include exploding a nuclear device close to the asteroid, impacting it at high speeds using a spacecraft, and gently nudging it on a new course using the gravitational attraction from a spacecraft hovering nearby.[1] The latter technique, known as a "gravity tractor", is especially attractive for situations where there is a long lead time between the detection of a potential threat and the date of Earth impact.

In order to execute a gravity tractor mission, a spacecraft must hover a short distance (typically on the order of a few hundred meters) from the surface of the asteroid, using ion engines to maintain altitude. The engines must be canted so that the exhaust plume doesn't impact the asteroid, negating the effects of the gravity tractor. Since this technique has never been performed, it is desirable to demonstrate its feasibility prior to use for an actual deflection. The proposed Asteroid Redirect Robotic Mission (ARRM) was slated to perform this demonstration as a secondary goal on the asteroid 2008EV5, following its primary goal of picking up a boulder from the surface. The combined spacecraft plus boulder mass could range up to 20 tons, and with hover times from 30-90 days, would provide enough mass to appreciably deflect the asteroid from its original trajectory. Measurement of the deflection would be accomplished by using the spacecraft as a radio beacon, or leaving a small radio beacon behind, orbiting or hovering at a relatively large distance from the asteroid, for some period of time. Two questions arise from this: 1) how long does the tractoring need to take place to make a measurable deflection, and 2) how long does the beacon need to remain in the asteroid vicinity to measure the deflection at a significant level of signal to noise.

* Supervisor, Outer Planet Navigation Group, Mission Design and Navigation Section, Jet Propulsion Laboratory, California Institute of Technology, Pasadena, California, MS 264-820, 4800 Oak Grove Dr., Pasadena, CA 91109.

In this paper, an attempt to answer these questions was performed using simulated data for a sample scenario involving ARRM. First, however, some background and general concepts of determining the orbits of asteroids from ground-based data is introduced. Then, details of how an orbiting spacecraft is used to dramatically improve on the ground-based approach is provided. Finally, the factors which influence how accurately the deflection can be measured are quantified and results using the ARRM scenario are presented.

ASTEROID AND SPACECRAFT ORBIT DETERMINATION

In order to mount any mission that involves getting near an asteroid, a reasonably accurate knowledge of where the asteroid is at any given time is needed. Preliminary estimates of the asteroid ephemeris are provided through ground-based observations of the asteroid, primarily astrometric data from optical telescopes, but also in a limited number of cases from radar bounces off the asteroid.[2] The accuracy of this method is dependent on many factors including the density, quality, resolution, and geometry of the observations, the orbital characteristics of the asteroid, and the length of time of the observation span. For optical astrometric data, the observations are brightness centroids of the asteroid against the background stars; the stars enable the precise determination of the inertial pointing direction of the camera, and the brightness centroid provides the Right Ascension (RA) and Declination (DEC) of the asteroid. Depending on the asteroid, the time span can be as short as a few days to weeks, or centuries as is the case for the larger well known ones. The second type of data, radar reflections, are obtained from large radar dishes, such as Arecibo in Puerto Rico or the 70 m dish at Goldstone, CA. These provide measurements of the range to the asteroid from the station. The accuracy of the measurement falls off rapidly with range, and in general, is only practical when the asteroid is within about 0.1 au of the Earth. The accuracy of this technique depends on which antenna is used and the distance; typical numbers from Arecibo are around 15-150 m, 1σ. Thus, although a very powerful measurement, only a small amount of asteroids have been observed this way. For asteroids which pass near the Earth however, this is a viable method to get high accuracy data on the ephemeris without needing to send a spacecraft to it.

Unlike ground-based asteroid orbit determination, the data for computing a spacecraft's orbit relies heavily on radiometric tracking data. These data are obtained from one or more of the antennas located at the three Deep Space Network (DSN) facilities located in Goldstone, CA, Madrid, Spain, and Canberra, Australia. In addition, antennas operated by the European and Japanese space agencies are sometimes used when the DSN antennas are busy. The three data types used are two-way Doppler, two-way range, and Delta-Differential One-way Range (DDOR). For two-way Doppler, the antenna sends a radio signal to the spacecraft which is coherently transponded and returned to Earth. The Doppler shift of the received signal measures the line-of-sight velocity of the spacecraft relative to the tracking station. After post processing to correct for systematic errors caused by the radio propagation through the atmosphere, the point-to-point random noise in the data is on the order of 0.1 to 0.2 mm/s (1σ), assuming a 60 second count time (for X-band data). For two-way range, the antenna sends a code which is transponded and returned. The time it takes between the transmit and receive time of the code measures the line-of-sight range from the station to the spacecraft. After accounting for atmospheric effects and the delays caused by transmission of the signal from the antenna phase center to the signal processing electronics, the random noise level is on the order of 2-4 m for each pass of data, where a pass can vary from 6-12 hours. The final data type, DDOR, is an interferometric data type, where the one-way signal transmitted from the spacecraft is received at two ground stations simultaneously. The time delay of the received signal between the stations measures the angular position of the spacecraft relative to the baseline formed from the line between the stations, and in the plane formed from the stations and the spacecraft. The angular accuracy of the measurement is dependent on the baseline length; for the Goldstone-Canberra baseline, the value is roughly 28 nrad per ns delay, and for the Goldstone-Madrid baseline, its about 36 nrad per ns. The noise level in the measurement is on the order of 0.2 ns (1σ). The metric accuracy then, is scaled by the distance of the spacecraft from the Earth.

For proximity operations around an asteroid, another data type is used: optical images of the asteroid from a camera onboard the spacecraft. In particular, a spacecraft near a small body uses many images of the body to first build a detailed shape model. With the shape model, combined with accurate estimates of the rotation rate and orientation body, surface features can be used to perform terrain-relative navigation (TRN). This technique has been used on several small body missions, such as Dawn[3] and Rosetta.[4] TRN effectively ties the spacecraft to the body, with accuracies depending on the resolution of the shape model and the distance; for orbits within 10 km as was the case for Rosetta, the spacecraft orbit can determined to the tens of m level with respect to the body.

Mathematically, the method used to process all the data (radiometric, ground and spacecraft optical) is a least squares fit of the data to dynamic models describing the orbits of the asteroid and/or spacecraft. Details of the statistical orbit determination method can be found in Reference 5; it will described briefly here. First, the 2nd order differential equations which describe the orbit are numerically integrated. The force models include gravitational perturbations from all the planets (including the Earth's moon), solar radiation pressure and propulsive events (for the spacecraft). In close proximity of the asteroid, the non-sphericity of the asteroid's gravity field is also modeled in the form of spherical harmonics to model the spacecraft motion around the asteroid.[5] For long term, high accuracy modeling of the asteroid's heliocentric motion, gravitational perturbations from the 15-20 largest asteroids are also included in the force model. One other force should also be mentioned with regards to modeling asteroid orbits, the Yarkovsky effect.[6] This is a small acceleration acting on the asteroid caused by thermal re-radiation as the sunward side of the asteroid heats up, then radiates the energy away as the face goes into darkness with its diurnal rotation. Because it is a very small effect, only a small handful of asteroids has quantified the magnitude of the acceleration caused by the Yarkovsky effect. Nevertheless, it should be accounted for when trying to measure the deflection from a gravity tractor.

With the motion of the asteroid and/or spacecraft integrated, predicted values of the data can be computed. These are then subtracted from the actual observed data to form residuals. If the initial conditions and models describing the motion were perfect, then the residuals should have zero mean with random noise fluctuations. This is never the case, however, so the least squares process adjusts the initial conditions and parameters of the models until converged. As a result, the best fit trajectory of both the spacecraft and/or asteroid are obtained.

Tracking a spacecraft near an asteroid provides the crucial third leg of the triad needed for high accuracy determination of an asteroid orbit if/when direct radar measurements of the asteroid are not available. The first leg of the triad is the ground-based optical observations of the asteroid, which gives the heliocentric asteroid orbit. The second leg is radiometric tracking of the spacecraft to obtain its heliocentric orbit. With TRN anchoring the spacecraft to the asteroid, tracking the spacecraft is effectively the same as tracking the asteroid, accurate to the level of the knowledge of the spacecraft's orbit relative to the body. Thus, the spacecraft range is a proxy for directly measuring the range to the asteroid from ground radars, and is roughly comparable in accuracy.

The least-squares fit process also provides the error estimate in the orbit determination; an important factor to consider when measuring the deflection from a gravity tractor. This error estimate, is provided as a fully correlated covariance matrix, $\mathbf{P}$, on the inertial, heliocentric Cartesian state of the asteroid at a specified epoch. Also from least-squares estimation theory, the covariance matrix can include not just the contribution from the parameters estimated in the filter but "consider" parameters as well. These are parameters which are in practice difficult to estimate, but whose errors also contribute to the uncertainty in the state. Mathematically, if $\mathbf{P_x}$ is the covariance of the estimated parameters, $\mathbf{P_c}$ is the covariance of the consider parameters, and $\mathbf{S_{xc}}$ is the sensitivity of the estimated parameters to the consider parameters, the total consider covariance P can be written as:[5]

$$\mathbf{P} = \mathbf{P_x} + \mathbf{S_{xc}} \mathbf{P_c} \mathbf{S_{xc}^T} \tag{1}$$

Thus, the consider parameters inflate the covariance of the state, but the uncertainties in the consider parameters are not improved. Certain consider parameters make a significant difference in the asteroid state error estimate, as will be seen later.

The diagonals of the matrix $\mathbf{P}$ are the square of the 1σ uncertainties on each position and velocity component of the state, but the correlations in the off-diagonal terms are important because they describe the shape of the error ellipse. Typically, the error ellipse for asteroids is elongated along its velocity direction, with the directions radial from the Sun and out-of-plane from the orbit plane being smaller. Since this geometry provides a more intuitive view of the uncertainty ellipse, P is generally rotated into the radial-transverse-normal (RTN) coordinates via the following rotation matrix:

$$\begin{aligned} \mathbf{R} &= \mathbf{r}/|\mathbf{r}| && (2)\\ \mathbf{T} &= \mathbf{N} \times \mathbf{R} && (3)\\ \mathbf{N} &= \mathbf{r} \times \mathbf{v}, && (4) \end{aligned}$$

where $\mathbf{r}$ and $\mathbf{v}$ are the three components of position and velocity in the inertial cartesian coordinate system, respectively. The rotation matrix, $\mathbf{M}$ is then:

$$\mathbf{M} = \begin{bmatrix} \mathbf{R} \\ \mathbf{T} \\ \mathbf{N} \end{bmatrix}, \tag{5}$$

and the inertial covariance $\mathbf{P}$ is rotated into $\mathbf{P'}$, the RTN frame by:

$$\mathbf{P'} = \mathbf{M} \mathbf{P} \mathbf{M^T}. \tag{6}$$

Furthermore, it is also useful to map forward the covariance matrix at the epoch time, t_0,to any time t in the future. This is accomplished using the state transition matrix, $\mathbf{\Phi(t)}$, which is defined as:

$$\mathbf{\Phi(t)} = \left[\frac{\partial (\mathbf{X})(\mathbf{t})}{\partial \mathbf{X}(\mathbf{t_0})} \right], \tag{7}$$

where vector $\mathbf{X}$ contains the three position and velocity components of the state vector, and the partial represents the sensitivity of the state at time t to the state at the epoch time. The covariance at any time, t, can be obtained then as

$$\mathbf{P_t} = \mathbf{\Phi} \mathbf{P} \mathbf{\Phi^T}. \tag{8}$$

$\mathbf{\Phi}$ can be compute numerically using finite differences, or as is typically done, integrated along with the state using standard least squares estimation techniques.[5] With the above two equations, the covariance can be rotated and mapped into RTN coordinates for any time before or after the epoch of the solution.

In general, the accuracy of the asteroid orbit from ground-based astrometric observations alone will vary greatly, ranging from many 10s to many 100s of km. Specifically, the case for the ARRM target, asteroid 2008EV5, was examined. Currently, 993 ground based astrometric observations from 2008-2010 is available, and has been used to determine the orbit and its associated covariance.[7] The mapped 1σ uncertainties for the time span June 2023 to June 2024, in heliocentric RTN coordinates, are plotted in Figure 1. Here, the inflation in the transverse component can be clearly seen, with values ranging from about 600 to 700 km over an 8 month time span. The radial and normal components are much smaller, but with higher variations. The radial uncertainty drops as low as a few km to a high of around 60 km. The normal component, perpendicular to the plane of the orbit, is always the best determined component; for 2008EV5, the values range from around 2-5 km over the time span. In Figure 1(b), it can be seen that the radial velocity is the least known, with values on the order of 10-20 cm/s. The transverse and normal components are in the sub to several mm/s range.

When a spacecraft is operating near the asteroid, the determination of the asteroid's orbit can be accomplished one of two ways. The first is the one practiced by the mission Navigation Teams to provide near real-time trajectory updates needed to fly the mission. All the radiometric and optical images of the asteroid taken by the spacecraft are processed together in the least-squares fit, simultaneously estimating the spacecraft and asteroid orbit. The initial guess of the asteroid ephemeris is the solution from the ground astrometry. This astrometry data is not used in the combined fit; instead, the information content of the data is embedded in the covariance matrix from that estimate (whose uncertainty is shown in Figure 1). This is used as an *a priori* condition to constrain the update of the orbit. Care must be taken when using this *a priori*, however, as it may overconstrain the correction to the orbit, resulting in a poor fit to both the spacecraft and asteroid.

The second method is used by the mission's Radio Science Team, post processing the data after the fact, and is described in detail in Reference 8. Here, the orbits of the asteroid and spacecraft are not estimated simultaneously. Instead, using the best fit spacecraft orbits for the duration of the mission, the range data to the spacecraft are shifted to the center of mass of the asteroid; this is equivalent to having a direct range measurement of the asteroid from the Earth. These data are combined with the long term ground astrometry to improve the orbit. This method has the advantage of being able to differentially weight the optical and pseudo-range observations to provide a more optimal fit, which cannot be done using the first method. This is also the preferred method for determining any gravity tractor deflection.

An example of the improvement using a spacecraft as a beacon near an asteroid is shown in Figure 2 for 2008EV5. These show the asteroid uncertainty in RTN coordinates assuming a spacecraft stay time from June 2023 to November 2023, a little over 6 months. As can be seen, the tens to hundreds of km uncertainty from ground observations only has been reduced by orders of magnitude. The radial uncertainties are now less than 200 m, and the other two components are less than a km. The velocity uncertainties have decreased to the mm/s or less value. These levels are now small enough where the change in the asteroid orbit from gravity tractoring is detectable.

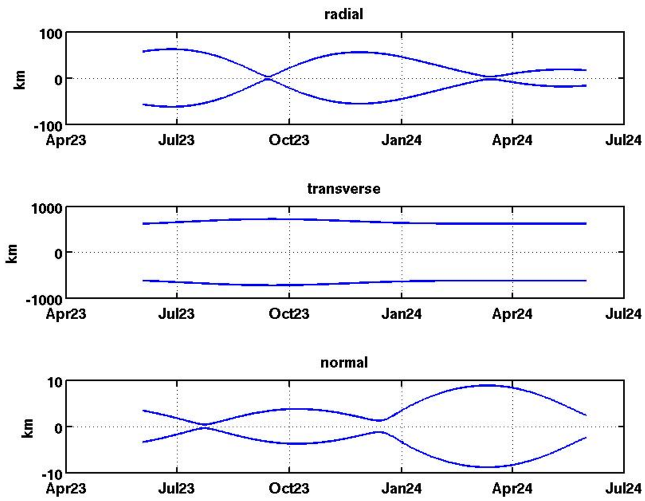

(a) RTN Position Uncertainty (1σ)

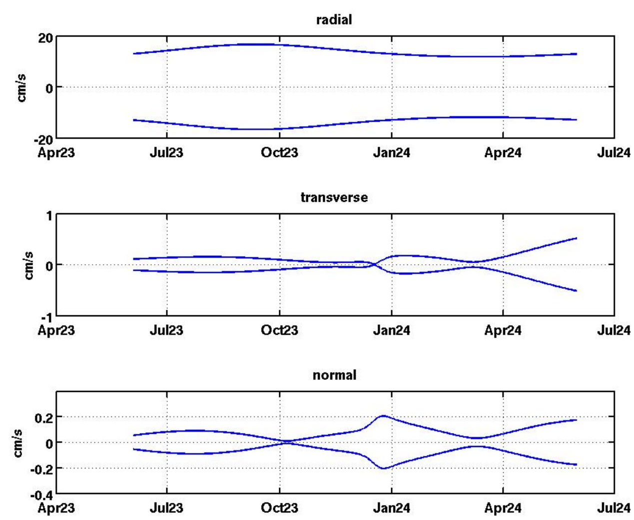

(b) RTN Velocity Uncertainty (1σ)

Figure 1. 2008EV5 Position and Velocity Uncertainties From Ground-based Astrometry

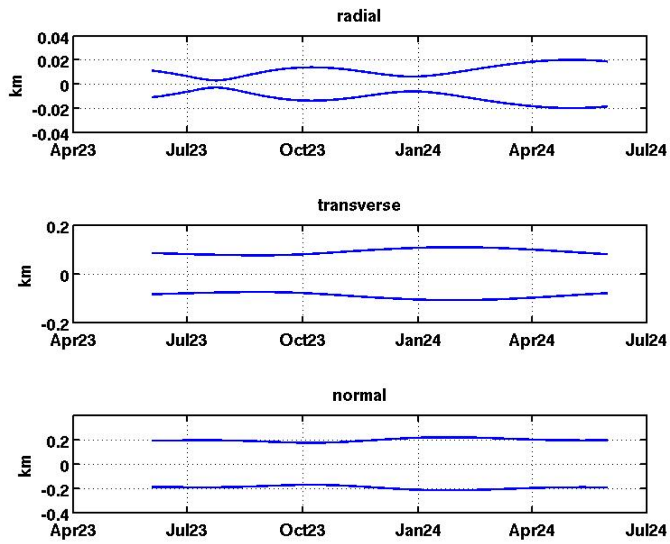

(a) RTN Position Uncertainty (1σ)

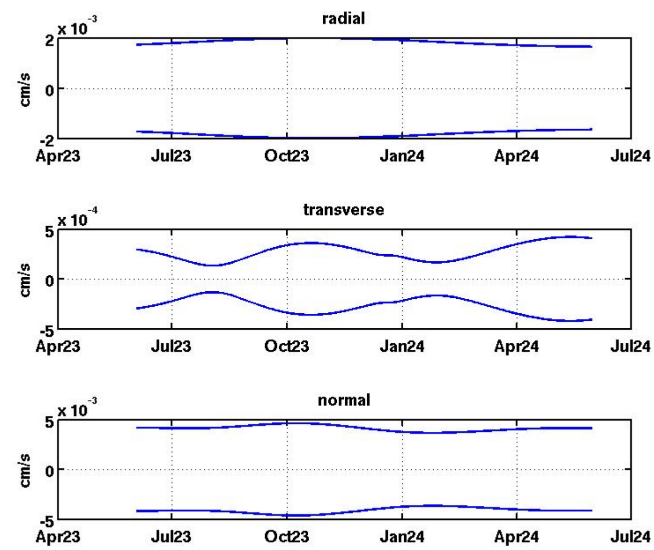

(b) RTN Velocity Uncertainty (1σ)

Figure 2. 2008EV5 Position and Velocity Uncertainties Including Spacecraft Tracking Data

ASTEROID GRAVITY TRACTOR DEFLECTION

The gravity tractor method relies on a spacecraft "hovering" near an asteroid using low-thrust ion engines to maintain a near constant altitude over the surface, preferably in the direction (or anti-direction) of the asteroid's velocity vector, and preferably applied near perihelion, for maximum effect. The amount of acceleration imparted to the asteroid depends on the hover altitude and direction, and the mass of the spacecraft. The acceleration values will vary slightly as the altitude and direction cannot be perfectly maintained. The details of the control of the spacecraft to maintain the hover are beyond the scope of this paper and are addressed elsewhere.[9] Here, a constant acceleration is imparted to the asteroid over a specified time period; the nominal acceleration values are those using representative spacecraft masses and hover strategies from the ARRM mission.

Figure 3 shows the actual deflection on 2008EV5 due to gravity tractoring; the coordinates shown here are in Earth-centered RTN frame for reasons described below. The acceleration imparted to the asteroid was 5.7 x 10^{-12} m/s^2, operating over the period December 21, 2023, to January 20, 2024 (30 days), along the asteroid velocity vector. The red line in the plots is the difference between the perturbed and undeflected trajectory of the spacecraft for both position and velocity. Also shown in blue are the 3σ uncertainties of the asteroid orbit estimate in the same reference frame. This plot shows that the change in the asteroid orbit takes considerable time to rise above the background knowledge of the orbit, indicating the difficulty in detecting the change.

Before quantifying numerically the signal to noise ratio of the detection, it is instructive to qualitatively get an understanding of the measurement being made. In order to do this, note that the tracking data obtained is not from the Sun, but from the Earth. Thus, the plots in Figure 3 are shown in an Earth-centered RTN frame, which also forms a natural coordinate system for the three types of tracking data used to measure the deflection. First, consider range data, which is directly along the Earth to asteroid (when the spacecraft is very near to it) radial direction and is thus aligned with the radial component in Figure3(a). The +/- 3σ range noise, around 10 m which is slightly conservative for X-Band data, is small on the scale, and clearly, the deflection level is above the noise level of the data itself very rapidly, although not above the overall uncertainty in the asteroid ephemeris knowledge.

For DDOR data, the two baselines formed by Goldstone-Canberra and Goldstone-Madrid form nearly orthogonal directions to observe angular shifts in the plane-of-sky. Although these are not aligned exactly with the RTN frame, the T and N components are roughly equivalent to illustrate the point. The noise of the DDOR data is around 0.6 ns (3σ) in the measurement of the signal delay, equivalent to 16.8 nrad for the Goldstone-Canberra and 21.6 nrad for the Goldstone-Madrid baselines, respectively. If this is multiplied by the range to the spacecraft, which for this example ranges from 0.1 to 0.6 au, the noise in metric units is obtained and amounts to roughly 300 - 1800 m over the time frame in the plots. From transverse and normal component plots in Figure3(a), it can be seen that it takes many months for the signal of the deflection rise above the noise level in the data.

Doppler data measures the velocity in the Earth-centered radial direction, aligned with the radial direction in Figure3(b). The 3σ noise is around 0.3 mm/s. This plot shows that the change in velocity is extremely small, less than 0.04 mm/s, and so is well below the random noise in the Doppler data. So, ultimately, the gravity tractor's effect on the asteroid's velocity is not directly measurable, and the change in range is what provides the signal of the deflection.

To summarize, the radiometric tracking data is used to precisely determine the spacecraft orbit,

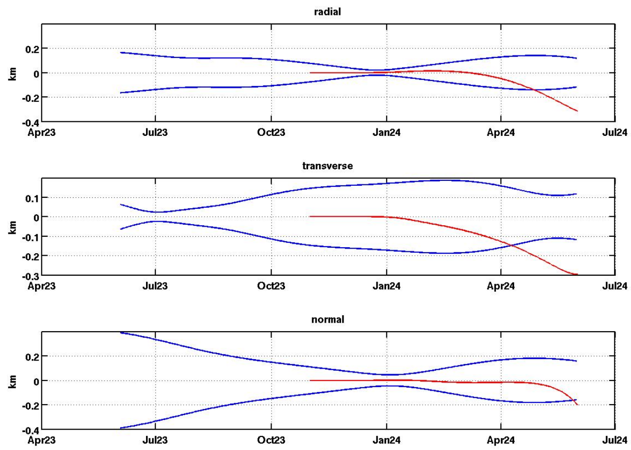

(a) Deflection in RTN Position

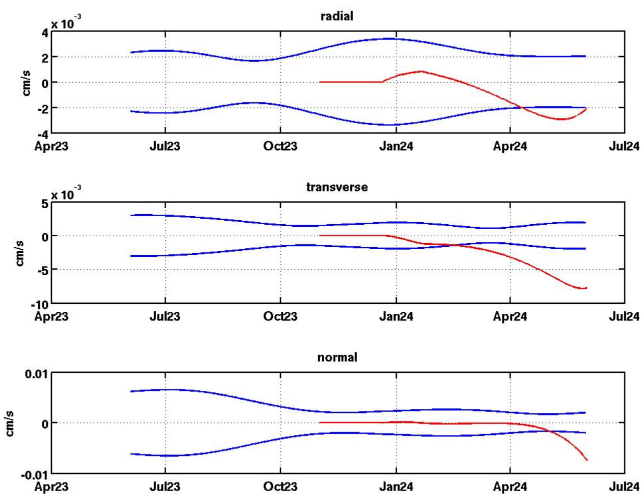

(b) Deflection in RTN Velocity)

Figure 3. Deflection of 2008EV5 in Position and Velocity From Gravity Tractor Spacecraft. The blue lines indicate +/- 3σ uncertainties, the red line shows the deflection.

which combined with onboard optical data of the asteroid, ties the two together. Then, the best fit orbit of the spacecraft is used to measure the change in the radial position of the asteroid as seen from the Earth. The level of measurability will now be quantified.

COVARIANCE ANALYSIS OF DETECTION

The process used to precisely quantify the detectability of the deflection is standard linear covariance analysis, which uses simulated data to obtain the asteroid state covariance matrix shown in Eqn. 1. As described above, tracking a spacecraft in the proximity of the asteroid is essentially equivalent to tracking the asteroid with range measurements. Thus, for simplicity, a covariance analysis is performed solely on the asteroid using simulated data from a tracking station to the asteroid. For the time period of interest, the equations of motion of the asteroid are numerically integrated. Simulated range measurements are then created and used to estimate the asteroid state, plus the tractor acceleration, with an *a priori* sigma set at 100% of the nominal value. Consider parameters are also used to get realistic values for the covariance; these include Earth orientation parameters (X and Y polar motion and UT1 time bias), media calibrations (Wet/Dry Troposphere delays, Day/Night ionosphere delays), DSN station locations, and the ephemeris of the Earth/Moon barycenter. Table 1 lists the complete set of estimated and consider parameters used in the filter, along with their *a priori* uncertainties.

In the course of performing the analysis, it was discovered that the Earth/Moon barycener ephemeris uncertainty was the consider parameter with the largest effect on the ability to measure the gravity tractor acceleration. This is not entirely surprising; since the goal is to measure the heliocentric motion of the asteroid, the orbital accuracy of the platform the measurements are made from, the Earth, makes a difference. Thus, a brief background on the heritage of the values used for the uncertainty of this parameter is given.

For NASA planetary missions, the planetary ephemerides are provided by the Solar System Dynamics (SSD) group at the Jet Propulsion Laboratory. Based on fitting centuries of astrometric observations, plus ranging measurements to spacecraft that have visited the planets, the numerically integrated orbits of all the planets are disseminated with the label Development Ephemeris (DE) nnn, where nnn is a 3 digit value designating a particular solution. Typically, these ephemerides are released for specific planetary missions. For example, the latest is DE 436 for use by the Juno mission. Along with the planet's orbit, the uncertainty on the orbit is also provided, with the formal covariance of the fit scaled by a value determined heuristically to match the observed variation in the observation residuals. For this analysis, a special covariance for the Earth/Moon barycenter ephemeris was obtained which best represents the current estimate of the Earth orbit uncertainty, which was scaled by 2 to approximate what the value will degrade to at the time frame of the mission, assuming no new measurements (labeled "CBE" for Current Best Estimate).[10] However, since it is reasonable to assume that future missions, such as Mars 2020, will provide more data in the future to improve the Earth ephemeris knowledge, a variation used scale factor of 1 to represent future levels of uncertainty.

The setup used for the simulations is the nominal ARRM scenario, which has a spacecraft arrival at 2008EV5 on June 20, 2023, start of gravity tractoring on December 7, 2023, and departure from the asteroid on January 21, 2024 (the baseline scenario). A second scenario was also studied, with a later arrival on March 2, 2024, start of gravity tractoring on August 25, 2024, and departure from the asteroid on September 25, 2024 ("late arrival" scenario).

Table 1. Filter Parameters

Estimated Parameter	A Priori Uncertainty(1σ)	Comment
Asteroid Position	270 x 620 x 40 m .	Inertial Cartesian values from *a priori* covariance at epoch in an Earth Mean Orbital 2000 coordinate frame
Asteroid Velocity	14.2 x 6.3 x 1.8 cm/s	Inertial Cartesian values from *a priori* covariance at epoch
Tractor Acceleration		5.7 x 10^{-12} m/s^2
Consider Parameter		
Polar Motion X and Y	1.7 x 10^{-5} deg	
UT1 Bias	0.75 msec	
Dry Troposphere Delay	1 cm	
Wet Troposphere Delay	4 cm	
Day Ionosphere Delay	55 cm	
Night Ionosphere Delay	15 cm	
DSN Station Location	*	Values from fully correlated covariance
Earth Barycenter Ephemeris	*	Values from fully correlated scaled covariance (see text)

The range data was simulated at a rate of three 8 hour long passes per week during the period of spacecraft arrival at the asteroid to the start of gravity tractoring. When the spacecraft is performing the tractoring, no data was assumed. Then, after the tractoring is completed, data is again simulated at a 3 passes per week cadence until the departure of the spacecraft. Also for this particular scenario, 2008EV5 is close enough to be trackable by ground radar (using either the Arecibo or Goldstone 70 m dish) at 2 times: July 1, 2024 - July 19, 2024, and April 10, 2025 - May 12, 2025. Thus, for the first scenario, ground radar is available after the tractoring period on two opportunities; for the second scenario, only the last opportunity. The significance of this is that the ground radar can be used in place of a spacecraft and thus allows the spacecraft to depart sooner after tractoring if needed. For data weighting, for the psuedo-spacecraft range, the noise was assumed to be 5 m (1σ); for the ground-based radar range, for July 2024 and April 2025 a vallue of 75 m and 150 m (1σ), respectively, was used.

Since the goal of this analysis is to determine how well the imparted acceleration on the asteroid (the "signal") can be detected compared the noise level on that signal, a good metric is the signal-to-noise ratio, S/N. For a given spacecraft mass and hover distance from the center of the asteroid, the nominal acceleration can be easily computed. For the covariance analysis, the *a priori* 1σ uncertainty was set to the nominal acceleration. The post-fit uncertainty, using data before and after tractoring, provides the noise level on the measurement, so the S/N value is simply the *a priori* divided by the postfit sigma on the acceleration. The minimum value of S/N to conclude that the deflection has been measured is difficult to define. Although in principle, S/N of 3 gives 99% confidence (for a scalar variable), in practice, there are many error sources which are difficult to model (such as solar plasma effects on the tracking data, ummodelled spacecraft accelerations due to spacecraft outgassing), and therefore are not accounted for in the covariance analysis, resulting in the formal statistics being overly optimistic. Thus, a somewhat large S/N value of around 10 was chosen as being the minimum for unambiguously detecting the tractoring acceleration signal.

RESULTS

The first goal was to see how long after the tractoring a spacecraft or beacon must remain in order to get a meaningful detection of the deflection. For the baseline reference trajectory, this result is shown in Figure 4 where the S/N of the detection is plotted against tracking time after the end of the tractoring period. The curve in red assumes the CBE Earth ephemeris uncertainty while the blue line shows it for the future assumed uncertainty level. In both cases, the tractoring duration was assumed to be 30 days at a value of 5.7 x 10^{-12} m/s^2, for a net ΔV of 0.015 mm/s imparted to the asteroid. This specific acceleration value was used because it was the baseline assumption for ARRM, given its spacecraft plus boulder mass of 20 tons, hovering in a halo-type orbit a few hundred m from the asteroids surface. Using the criteria of 10 for the minimum S/N for detection, this occurs at roughly the 160 day mark using the CBE Earth ephemeris, and about 90 days for the future Earth ephemeris. These results are promising in that it does not take an unrealistically long stay at the asteroid, especially with expected improvements in Earth's ephemeris knowledge, to get a reasonable detection. It is also interesting to note that the improvement in S/N flattens out for both cases a little after 300 days at values of 15 and 30.

Figure 5 shows an alternate scenario where the detection is done by ground radar measurements and assuming no post-tractoring measurements by a proximity spacecraft. As described above, these opportunities occur in July 2024 and April/May 2025. From the plot, it can be seen that the ground radar measurement is not sufficient to meet the S/N criteria for CBE Earth, and just at the

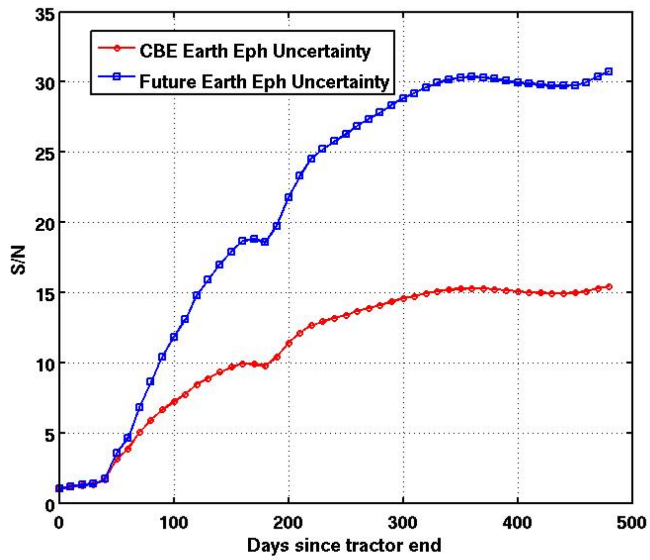

Figure 4. S/N **vs Post-tractor Tracking Duration**

threshold for the future Earth case, after the first opportunity. Both cases are sufficient after both sets of ground radar measurements are made, and although neither match the results assuming a proximity spacecraft, they are good enough to claim detection has been made.

The second goal was to examine the sensitivity of the deflection measurement to the net ΔV imparted by the tractor. The net ΔV was used as a free parameter because it can be accomplished any number of ways, varying any combination of stay time, spacecraft mass, and hover distance from the asteroid; in this analysis the stay time was varied from 5 to 40 days to get the range of ΔVs. In Figure 6, the S/N values for the baseline trajectory, evaluated with 6 and 12 months of post-tractoring beacon tracking, and using the future Earth ephemeris uncertainty, are plotted as a function of the net ΔV. Here, it can be seen that the sensitivity to ΔV is fairly linear. Doubling the ΔV approximately doubles the S/N, with the slope slightly steeper when evaluated at 12 months vs 6. Furthermore, the result underscores that very small ΔVs imparted to the asteroid below the detectability of Doppler has a cumulative effect that is clearly detectable above the background after a reasonable length of time.

The final goal was to look at the sensitivity of the results to the time frame of the operations. Thus, the same analysis for the late arrival trajectory was performed. Figure 7 plots the S/N vs tracking time for this scenario, which is both qualitatively and quantitatively different than the baseline reference trajectory. For one, the difference between using the CBE and future best Earth ephemeris uncertainty is not nearly as pronounced. Second, the curve shows relatively modest improvement for the first 130 days, then makes a dramatic rise between 130 and 160 days, after which it flattens out again. Third, the S/N after 6 months is a factor of 5-10 better, with most of this improvement happening in the 130-160 day period. The cutoff S/N of 10 is achieved after around 100 days for either ephemeris. As of this writing, the reason for the dramatic improvement is not clear and will need to be investigated. Also interesting to note is that for this scenario, the only ground radar measurement available is the April/May 2025 opportunity which occurs roughly

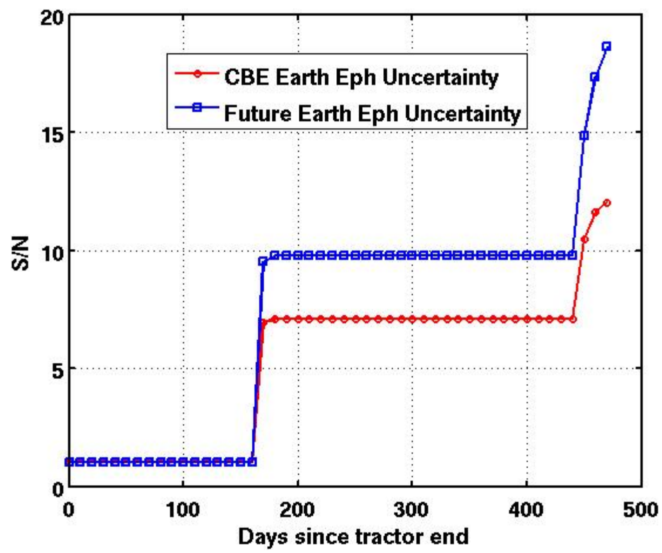

Figure 5. S/N **vs Post-tractor Ground Radar Observations**

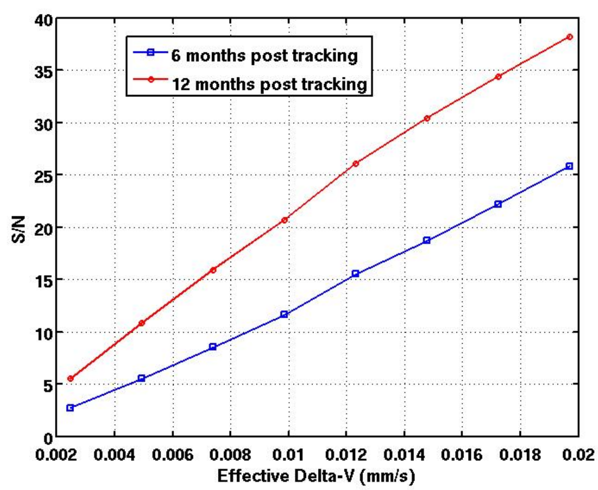

Figure 6. S/N **vs Accumulated Tractor** Δ**V**

180 days after tractoring. Even though this is after the knee in the curve in Figure 7, the S/N only reaches a value of 10 (plot not shown), indicating that the rapid improvement only occurs if the asteroid is continually tracked through this period.

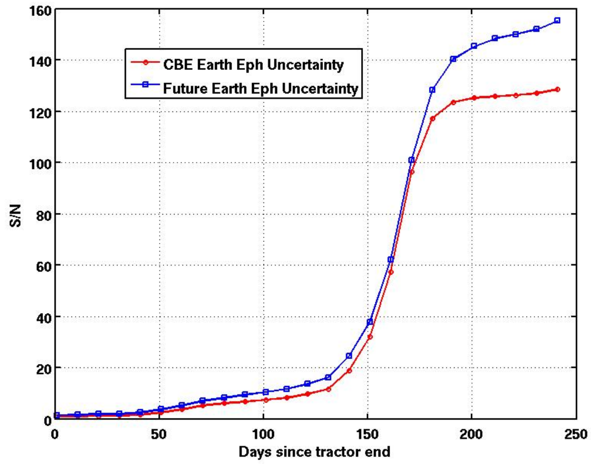

Figure 7. S/N **vs Post-tractor Tracking Duration for Late Arrival Trajectory**

Figure 8 shows the S/N vs net ΔV plot for this reference. Here, the S/N was evaluated at the 100 and 200 day mark, corresponding to a time prior to the dramatic improvement and a time after. For this time frame, performing the post-tractoring measurements for an extra 100 days makes a large difference in the measured S/N, where even the smallest ΔV imparted to the asteroid is detectable well above the background noise.

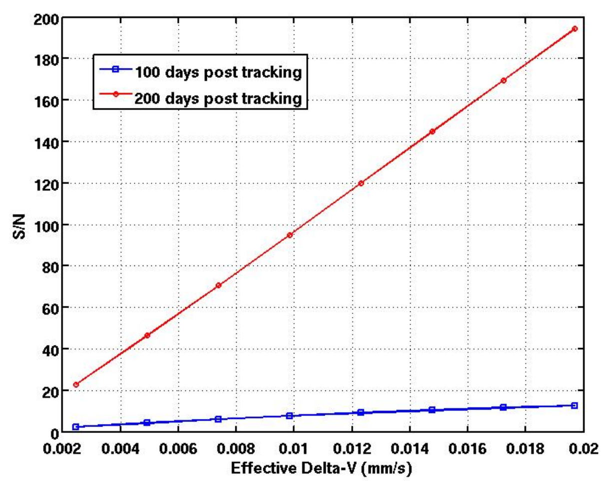

Figure 8. S/N **vs Accumulated Tractor ΔV for Late Arrival Trajectory**

SUMMARY AND CONCLUSIONS

In this paper, the capability to detect the acceleration imparted to an asteroid by a gravity tractor spacecraft was examined. Using a criteria that a S/N of 10 is the minimum needed to definitively claim that the acceleration was detected, it was found that tracking a spacecraft for 4-6 months after the tractoring is completed is the minimum necessary to achieve this goal. The results are quite sensitive, however, to several factors, including the assumption on the knowledge of the Earth ephemeris and the time frame for which the experiment takes place. Nevertheless, even when the value of the imparted ΔV is extremely small (less than 0.05 mm/s), the cumulative effect on the asteroid is detectable using range measurements to the asteroid. Furthermore, the range measurement does not have to be made from a spacecraft in proximity of the asteroid; direct ranging via ground radar is almost as effective, but with the caveat that the asteroid must make a reasonably close pass to the Earth.

Future work in this area would be to examine more closely why the measurement is so sensitive to the time frame, and the geometry which makes a specific time frame better than another. Finally, these results are specific to a demonstration mission for a gravity tractor. In a situation where the tractoring is done on an actual Earth impacting asteroid, the results may be dramatically different for several reasons, including the fact that such an asteroid's orbit would likely be very poorly determined initially, the stay time for tractoring would likely be much longer to guarantee that the asteroid is diverted from an impacting course, and the prediction time for determining the tractoring effect may be many years, even decades, past the tractoring time.

ACKNOWLEDGEMENTS

The research described in this paper was carried out at the Jet Propulsion Laboratory, California Institute of Technology, under a contract with the National Aeronautics and Space Administration.
Copyright (c) 2017 California Institute of Technology. U.S Government sponsorship acknowledged.

REFERENCES

[1] E. Lu and S. Love, "Gravitational tractor for towing asteroids," *Nature*, Vol. 438, November 2005, pp. 177–178.

[2] S. J. Ostro, "Planetary Radar Astronomy," *Reviews of Modern Physics*, Vol. 65, October 1993, pp. 1235–1279.

[3] B. Kennedy, M. Abrahamson, A. Ardito, R. Haw, N. Mastrodemos, S. Nandi, R. Park, B. Rush, and A. Vaughan, "Dawn Orbit Determination Team: Modeling and Fitting of Optical Data at Vesta," *AAS/AIAA Spaceflight Mechanics Meeting, Kauai, Hawaii*, February 10-14 2013. Paper AAS 13-347.

[4] S. Bhaskaran, S. Broschart, D. Han, N. Mastrodemos, B. Owen, I. Roundhill, B. Rush, J. Smith, D. Surovik, F. Budnik, and V. Companys, "Rosetta Navigation at Comet Churyumov-Gerasimenko," *AIAA Guidance and Control Conference, Breckenridge, Colorado*, February 2015. Paper AAS 15-122.

[5] B. Tapley, B. Schutz, and G. Born, *Statistical Orbit Determination*. San Diego, CA: Elsevier Academic Press, 1st ed., 2004.

[6] D. Farnocchia, S. Chesley, D. Vokrouhlicky, A. Milani, F. Spoto, and W. Bottke, "Near Earth Asteroids with Measurable. Yarkovsky Effect," *Icarus*, Vol. 224, 2013, pp. 1–13.

[7] HORIZONS *http://www.horizons.jpl.nasa.gov*.

[8] A. Konopliv, J. Miller, W. Owen, D. Yeomans, and J. Giorgini, "A Global Solution for the Gravity Field, Rotation, Landmarks, and Ephemeris of Eros," *Icarus*, Vol. 160, 2002, pp. 289–299.

[9] S. Broschart and D. Scheeres, "Control of Hovering Spacecraft Near Small Bodies: Application to Asteroid 25142 Itokawa," *Journal of Guidance, Control, and Dynamics*, Vol. 28, No. 2, 2005, pp. 177–178.

[10] W. Folkner *Personal communication*.